

## Anion Competition for a Volume-Regulated Current

Irena Levitan and Sarah S. Garber

Department of Physiology, Allegheny University of Health Sciences, Philadelphia, Pennsylvania 19129 USA

**ABSTRACT** We have examined whether the anionic amino acids, glutamate and aspartate, permeate through the same volume-regulated conductance permeant to  $\text{Cl}^-$  ions. Cell swelling was initiated in response to establishing a whole-cell configuration in the presence of a hyposmotic gradient. Volume-regulated anion currents carried by  $\text{Cl}^-$ , glutamate, or aspartate developed with similar time courses and showed similar voltage-dependent inactivation. Permeability ratios ( $P_{\text{aa}}/P_{\text{Cl}}$ ) calculated from measured reversal potentials were dependent on the mole fraction ratio (MFR) of the permeant anions ( $[\text{aa}]/([\text{aa}] + [\text{Cl}^-])$ ). MFR was varied from 0.00 to 0.97. As the fraction of amino acid increased,  $P_{\text{aa}}/P_{\text{Cl}}$  decreased. Current amplitude was similarly dependent on MFR. These results show that the permeation of anionic amino acids and that of  $\text{Cl}^-$  ions are not independent of each other, indicating that the ion channel underlying the volume-regulated conductance can be occupied by more than one ion at a time. Application of Eyring rate theory indicated that the major barrier to  $\text{Cl}^-$  ion permeation is at the intracellular side of the membrane, and that the major barrier to amino acid permeation is at the extracellular side of the membrane. The interactions between these permeant ions may have a physiological modulatory role in volume regulation through a volume-regulated anion conductance.

### INTRODUCTION

The osmotic environment surrounding mammalian tissues is normally maintained within a narrow range. Cells may be exposed, however, to osmotic stress during pathophysiological states such as edema, stroke, polydipsia, and diabetes (Law, 1994; McManus and Churchwell, 1994). Many cell types have developed mechanisms to respond to osmotically induced changes in volume to prevent cell death. Cells swell in response to acute exposure to an external solution that is hypotonic relative to the cytosol. Recovery from swelling is termed regulatory volume decrease (RVD) (Chamberlin and Strange, 1989; Deutsch and Lee, 1988; Hoffman, 1992; Law, 1991). The initial response to swelling is to reduce the intracellular concentration of  $\text{K}^+$  and  $\text{Cl}^-$  so that water will flow out of the cell, allowing the cell volume to return to normal. A volume-regulated current is thought to be the trigger that links cell swelling to the loss of  $\text{Cl}^-$  ions and subsequent volume recovery. The outward flow of  $\text{Cl}^-$  via this current then depolarizes the membrane, leading to the subsequent opening of voltage-gated  $\text{K}^+$  channels, allowing water to move out of the cell, and volume recovery.

Other anions may substitute for  $\text{Cl}^-$  in volume-regulatory processes. Glutamate and aspartate are among the most abundant amino acids ( $\sim 30$  mM), and changes in their concentrations in osmotically challenged cells make a significant contribution to adaptive osmoregulation, such as RVD (Law, 1991, 1994). Volume-regulated efflux of amino acids in response to cell swelling has been demonstrated in a variety of cells (Law, 1991). The rate of volume-regulated fluxes of amino acids depends linearly on their concentra-

tion up to 15–60 mM (Haynes and Goldstein, 1993; Kirk et al., 1992; Roy and Malo, 1992; Sanchez-Olea et al., 1991). The half-maximum values,  $K_m$ , for amino acid uptake by characterized amino acid carriers, however, are in the micromolar range (Storck et al., 1992). The difference between the flux rates and  $K_m$  values suggests that there are two distinct mechanisms of transport and has led to a hypothesis that the volume-regulated efflux of amino acids may be mediated by an ion channel rather than by a carrier protein (Kirk et al., 1992; Roy and Malo, 1992).

Organic osmolytes such as amino acids exist in anionic, neutral, and cationic forms under physiological pH. Three common intracellular amino acid osmolytes are taurine, glutamate, and aspartate (Law, 1991; Roy, 1995). Glutamate and aspartate are anionic at physiological pH, whereas taurine is without a net charge (the pK of taurine is 8.8) (Roy and Malo, 1992). The permeability of anionic and neutral amino acids in cells exposed to a hyposmotic stress is much higher than the permeability of the cationic amino acids such as lysine or arginine (Roy and Malo, 1992). Volume-regulated amino acid fluxes are also inhibited by chloride channel blockers 4,4'-diisothiocyanatostilben-2,2'-disulfonic acid and 5-nitro-2 (3-phenylpropylamino) benzoic acid (Haynes and Goldstein, 1993; Jackson and Strange, 1993; Kimelberg et al., 1990; Kirk and Kirk, 1993; Sanchez-Olea et al., 1991). These observations suggest that the same ion channel may be responsible for  $\text{Cl}^-$  and anionic amino acid permeation under hyposmotic conditions. An alternative explanation is that there are two types of ion channels, one that is responsible for swelling-induced  $\text{Cl}^-$  transport and another for amino acid transport, that have the same trigger for activation.

This study addresses the hypothesis that  $\text{Cl}^-$  and the anionic amino acids, glutamate and aspartate, may permeate through the same ion channel. We show here that 1) volume-regulated currents carried by  $\text{Cl}^-$ , glutamate, or aspar-

Received for publication 2 October 1997 and in final form 27 March 1998.

Address reprint requests to Dr. Sarah S. Garber, Department of Physiology, Allegheny University of Health Sciences, 2900 Queen Lane, Philadelphia, PA 19129. Tel.: 215-991-8408; Fax: 215-843-6516; E-mail: garber@auhs.edu.

© 1998 by the Biophysical Society

0006-3495/98/07/226/10 \$2.00

tate develop in myeloma cells after the cells are challenged with a transmembrane osmotic gradient; 2) currents carried by all three anions exhibit similar voltage-dependent inactivation; and 3) the permeation ratios vary with ionic composition, suggesting that the anions compete with each other for the same permeation pathway. These three lines of evidence support the hypothesis that the transport of  $\text{Cl}^-$  and anion amino acids uses the same permeation pathway under hyposmotic conditions.

## MATERIALS AND METHODS

### Tissue culture

Myeloma (RPMI 8226) cells, obtained from the American Tissue Culture Collection (Bethesda, MD), were grown in suspension with RPMI 1640 (Cell Grow of Fisher Scientific/Mediatech, Washington, DC) supplemented with 10% fetal bovine serum (Gibco BRL, Grand Island, NY). Cells were fed and split every 2–3 days. In preparation for recording, cells were washed twice with RPMI 1640 without sera. Cells were allowed to settle on a glass coverslip and washed with extracellular recording solution before recording.

### Solutions

Mole fraction ratios (MFRs) of  $\text{glut}/\text{Cl}^-$  or  $\text{asp}/\text{Cl}^-$  are defined as  $[\text{glut}]/([\text{glut}] + [\text{Cl}^-])$  or  $[\text{asp}]/([\text{asp}] + [\text{Cl}^-])$ . Extracellular MFR was varied between 0.00 and 0.97, whereas the respective MFR of the intracellular solution was maintained constant at 0.99. Complete replacement of  $\text{Cl}^-$  in the extracellular solution (MFR = 1.00) was not tolerated well by the cells or electrodes.

External recording solution at MFR of 0.00 contained (in mM) 150 NaCl, 1 EGTA, 2  $\text{CaCl}_2$ , 10 HEPES (pH 7.2). Extracellular MFR was varied by substituting NaCl with NaGlut or NaAsp. Internal solutions contained (in mM) 120 N-methyl-D-glutamine (NMDG)-Glut, 120 CsGlut, or 120 CsAsp and 10 HEPES, 4 ATP (pH 7.2) (NMDG-OH or CsOH) with free  $[\text{Ca}^{2+}] \approx 10$  nM (0.1  $\text{CaCl}_2$ , 1.1 EGTA). Intracellular solutions contained  $\text{Cs}^+$  or NMDG $^+$  to decrease the possible contamination of  $\text{Cl}^-$  outward current (inward flux) by outward cation currents. Chemicals were obtained from Fisher Scientific (Fairlawn, NJ) or Sigma (St. Louis, MO). The osmolarity of all solutions was determined immediately before recording with a vapor pressure osmometer (Wescor, Logan, UT) and was adjusted by the addition of sucrose, as required. Average osmolarities of external and internal solutions used to challenge cells were  $310 \pm 10$  mOsm and  $380 \pm 10$  mOsm, respectively.

### Recording

The current was activated by challenging cells with a transmembrane hyposmotic gradient of extracellular/intracellular osmolarity  $0.8 \pm 0.03$ . The gradient was created with membrane rupture and the initiation of the whole cell recording. Development of current was monitored with a 500-ms linear voltage ramp from a holding potential of  $-60$  mV to  $+100$  mV at an interpulse interval of 10 s.

The normal cellular current convention is used when referring to the direction of current. In other words, outward current refers to inward  $\text{Cl}^-$  ion flow. Ionic currents were measured using the whole-cell configuration of the standard patch-clamp technique (Hamill et al., 1981). Pipettes were pulled from N51A glass (Garner Glass, Claremont, CA), coated with Sylgard (Dow Corning Corp., Midland, MI), and fire polished to give a final resistance of 2–6 M $\Omega$ , using the above recording solutions. A NaCl agar bridge was used for a reference electrode. Currents were recorded with an EPC9 amplifier (HEKA Elektronik, Lambrecht, Germany) and accompanying acquisition and analysis software (Pulse and PulseFit; HEKA Elektronik) running on a Macintosh Quadra 700 or 800.

Liquid junction potentials between the pipette and the bath solutions were nulled immediately before seal formation. Values of the junction potentials were measured with a 3 M salt bridge. Values of liquid junction potentials for MFRs of 0.20–0.97 ranged between  $+1$  and  $+7$  mV relative to MFR = 0.00. These values are similar to liquid junction potentials estimated from a modified form of Henderson liquid junction potential equation as described by Barry and Lynch (1991), assuming that the mobilities of aspartate and glutamate are similar to the mobility of acetate. In the whole-cell configuration, correction for the junction potentials requires that the value of the junction potential will be subtracted from the uncorrected value (Barry and Lynch, 1991; Neher, 1992). Thus correction for liquid junction potentials shifts the uncorrected reversal potentials to more hyperpolarized values. In this paper, uncorrected values of reversal potentials are presented because the exact values of the amino acid mobilities are not known. Correction for the liquid junction potentials would increase the anomalous mole fraction behavior of the current.

Establishment of the whole-cell configuration may also cause the development of a liquid junction potential between cell cytoplasm and pipette solution. In small cells, such as myeloma cells (10–20  $\mu\text{m}$  in diameter), mobile ions equilibrate across the pipette orifice by diffusion within a few seconds, and a liquid potential between the cytoplasm and pipette solution goes toward 0.00 mV (Neher, 1992). Because of the presence of relatively large immobile anions, however, a potential between cytoplasm and the pipette may not be a simple liquid junction potential, but may include a Donnan potential. The peak of such a Donnan potential will occur immediately after seal rupture and is a function of the ratio between the total initial concentration of large “immobile” anions in the cell and the cation concentration in the pipette (Neher, 1992). The maximum value of  $-12$  mV was estimated for a peak Donnan potential, assuming that the total initial concentration of large “immobile” anions in the cell is equal to the cation concentration in the pipette (Barry and Lynch, 1991). All of the measurements shown here were performed with the same intracellular recording solutions. Because the Donnan potentials depend only on the intracellular solutions and not on the extracellular solutions, any Donnan potentials would be the same in each measurement and would have no effect on the mole fraction behavior of the current.

Pipette and whole-cell capacitances were automatically compensated. Whole-cell capacitance and series resistance ( $R_s$ ) were monitored throughout the recording. In recordings using cells with large current amplitudes ( $>500$  pA), series resistance compensation (95% compensation with a 100- $\mu\text{s}$  lag) was used. Occasionally, a lower percentage compensation was required to prevent current oscillation. Cells exhibiting small current amplitudes ( $<500$  pA) did not require series resistance compensation. In these cases, the voltage error involved was less than 5%. Results are based on records made from  $>150$  cells.

### Analysis

Voltage dependence of inactivation was determined using a modified h-infinity function (Levitan and Garber, 1995):

$$R = \frac{R_1 - R_2}{1 + e^{(V - V_{0.5})/k}}$$

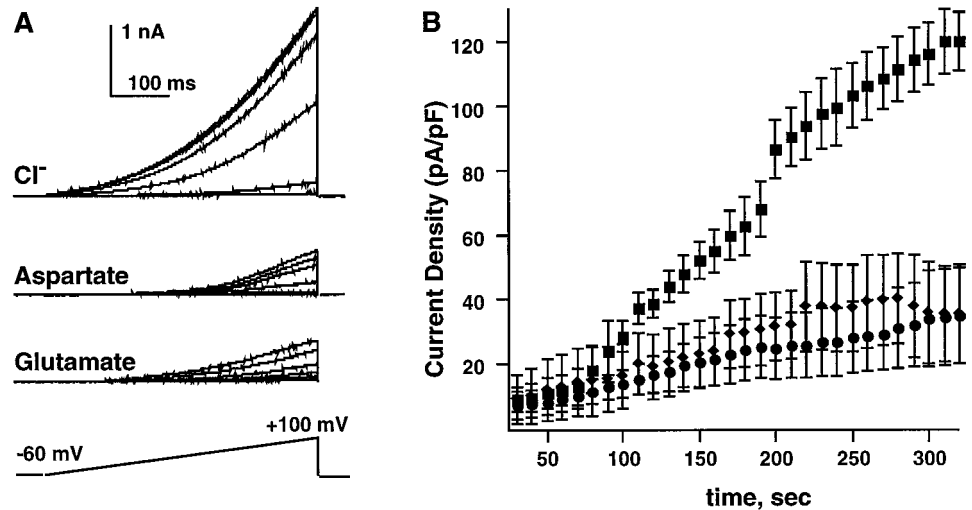
where  $R$  is the normalized ratio of the current amplitude ( $I_t$ ) in response to a test voltage pulse ( $V_t = +140$  mV) to that ( $I_c$ ) of a conditioning voltage pulse ( $V_c = -60$  mV to  $+140$  mV),  $V_{0.5}$  is the midpoint of inactivation,  $k$  is the slope factor,  $R_1$  is the inactivation ratio at 0 mV, and  $R_2$  is the minimum theoretical inactivation ratio at the highest voltage used for fit. Fits to data for the voltage dependence of inactivation were obtained with a Levenberg-Marquardt algorithm (Igor; WaveMetrics, Lake Oswego, OR).

Permeability ratios for  $P_{\text{asp}}/P_{\text{Cl}}$  and  $P_{\text{glut}}/P_{\text{Cl}}$  were calculated from measured reversal potentials, using the Goldman-Hodgkin-Katz (GHK) equation:

$$E_{\text{rev}} = \frac{RT}{zF} \ln \frac{[\text{Cl}]_i + (P_{\text{aa}}/P_{\text{Cl}})[\text{aa}]_i}{[\text{Cl}]_o + (P_{\text{aa}}/P_{\text{Cl}})[\text{aa}]_o}$$

where  $P_{\text{aa}}/P_{\text{Cl}}$  is the ratio of the permeability of the relevant amino acid to that of  $\text{Cl}^-$ .

**FIGURE 1** Activation of volume-activated anion currents carried by  $\text{Cl}^-$ , aspartate, or glutamate. (A) Families of currents elicited by linear voltage ramps from  $-60$  to  $+100$  mV recorded from the individual cells. The currents were recorded 30, 80, 130, 180, 230, and 280 s after whole cell configuration was established. (B) Average time courses for currents carried by  $\text{Cl}^-$  (■), aspartate (◆), or glutamate (●). Error bars represent SEM (number of cells  $\geq 5$ ).



Theoretical analysis of anomalous mole fraction behavior was performed on the basis of Eyring rate theory (Eyring et al., 1949), using "Barrier," a program developed by Dr. Ted Begenisch (Rochester University, Rochester, NY). "Barrier" simulates a four-barrier three-site permeation model. Mathematical details for a two-site version of this model can be found in Begenisch and Cahalan (1980), and some of the general properties of the three-site version can be found in Begenisch and Smith (1984), as described by Perez-Cornejo and Begenisch (1994).

## RESULTS

### Activation and inactivation of volume-regulated anionic currents carried by $\text{Cl}^-$ or anionic amino acids

Volume-regulated anion currents carried by  $\text{Cl}^-$ , aspartate, or glutamate are activated in myeloma cells challenged with

a transmembrane osmotic gradient. Currents produced by anionic amino acids have been observed previously in a number of cell types (Roy, 1995; Roy and Banderali, 1994). Fig. 1 shows that currents carried by  $\text{Cl}^-$ , aspartate, or glutamate develop gradually over a similar period of time after the establishment of a transmembrane osmotic potential. Note that the development of current carried by aspartate or glutamate is slower than that carried by  $\text{Cl}^-$ .

A characteristic feature of the volume-regulated  $\text{Cl}^-$  current is the development of voltage-dependent inactivation. Although voltage-dependent inactivation of the volume-regulated  $\text{Cl}^-$  is not likely to be physiological in nonexcitable cells (Levitan and Garber, 1995), it can be used as a comparative criterion for currents carried by  $\text{Cl}^-$  or anionic amino acids. The voltage-dependent inactivation of volume-

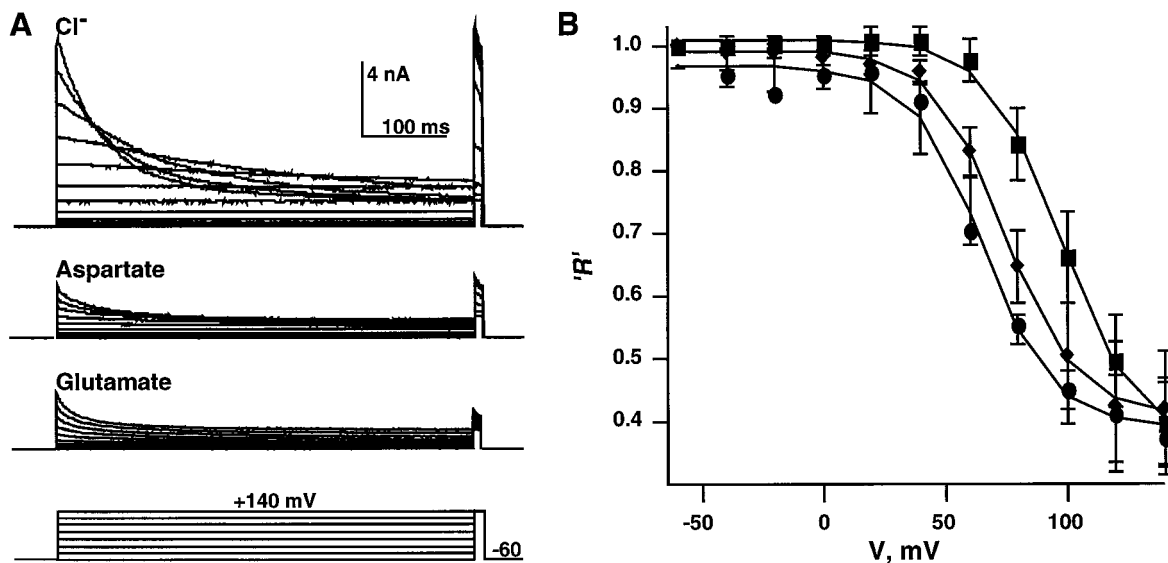


**FIGURE 2** Voltage-dependent inactivation of volume-regulated currents carried by  $\text{Cl}^-$  or by aspartate. (A) Volume-regulated current recorded in response to a family of voltage steps from  $-60$  to  $+140$  mV. The upper traces show a current family recorded from a cell exposed to  $\text{MFR} = 0.0$  (high extracellular  $\text{Cl}^-$ ), and the middle family of traces was recorded from the same cell when the extracellular solution was replaced with a solution of  $\text{MFR} = 0.97$  (high extracellular aspartate). The lower family was recorded from a different cell exposed to extracellular glutamate ( $\text{MFR} = 0.97$ ). (B) Voltage dependences of inactivation of currents carried by  $\text{Cl}^-$  (■), by aspartate (◆), or by glutamate (●) are similar. Current inactivation,  $R$ , is defined in Materials and Methods (number of cells  $\geq 5$ ).

regulated currents carried by  $\text{Cl}^-$  ions or anionic amino acids is shown in Fig. 2 *A*. A two-pulse voltage protocol with a conditioning pulse ranging from  $-60$  mV to  $+140$  mV, and a test pulse of  $+140$  mV was used. Voltage-dependent inactivation is apparent from accelerated decay of the anion current at large depolarization. The slope factor of the modified h-infinity function (Fig. 2 *B*) was similar, regardless of whether the current was carried by  $\text{Cl}^-$  ( $k = 15.1$ ), aspartate ( $k = 14.5$ ), or glutamate ( $k = 14.4$ ). The slope of current decay provides an index of the steepness of the sigmoid curve and can be interpreted as the movement of charge. The similarity between the slopes indicates that the same amount of charge is moved during voltage-dependent inactivation of the current carried by each anion. The midpoint of inactivation, however, shifted slightly to a less depolarized value in currents carrying either amino acid ( $V_{0.5} = 98, 75, 66$  mV for  $\text{Cl}^-$ , aspartate, and glutamate, respectively). This shift was less than that seen for volume-regulated chloride currents in different cell types (e.g., Levitan and Garber, 1995). The similarity of activation time courses and voltage-dependent inactivation suggests that  $\text{Cl}^-$  and anionic amino acids may use the same permeation pathway. A direct approach, however, to determining if  $\text{Cl}^-$  and anionic amino acids permeate through the same or different ion channels is to test whether these ions interact with each other during permeation through the channel pore.

### Interaction between permeant anions

Interaction between the permeant ions can be tested by measuring permeability ratios and current amplitude over a range of MFR. If the two ionic species use separate permeation pathways such as distinct ion channel species, ion permeation will be independent. In this case, the permeability ratios will be independent of the MFR of the ionic species, and current amplitudes will change linearly with the MFR of the ionic species (Hille, 1984). Deviation from these two rules of independence indicate that permeation of the two ionic species is not independent and that the ions may interact with each other while moving through the ion channel pore. Ion-ion interaction can only occur within an ion channel that can be simultaneously occupied by more than one ion at a time.

Asp:Cl<sup>-</sup> permeability ratios for volume-regulated anion current were calculated from the current reversal potentials. Reversal potentials of the current were determined for extracellular MFRs of asp:Cl<sup>-</sup> ranging from 0.00 (high extracellular Cl<sup>-</sup>) to 0.97 (low extracellular Cl<sup>-</sup>). Typical current-voltage relationships (*I-V* curves) for cells exposed to asp:Cl<sup>-</sup> MFRs of 0.40, 0.80, and 0.97 are shown in Fig. 3 *A*, *B*, and *C*, respectively. These *I-V* curves are compared to the *I-V* curves recorded at MFR = 0.00 from the same cells. In these experiments the currents initially developed when the cells were exposed to low extracellular MFRs. After the currents were fully developed, the extracellular solutions

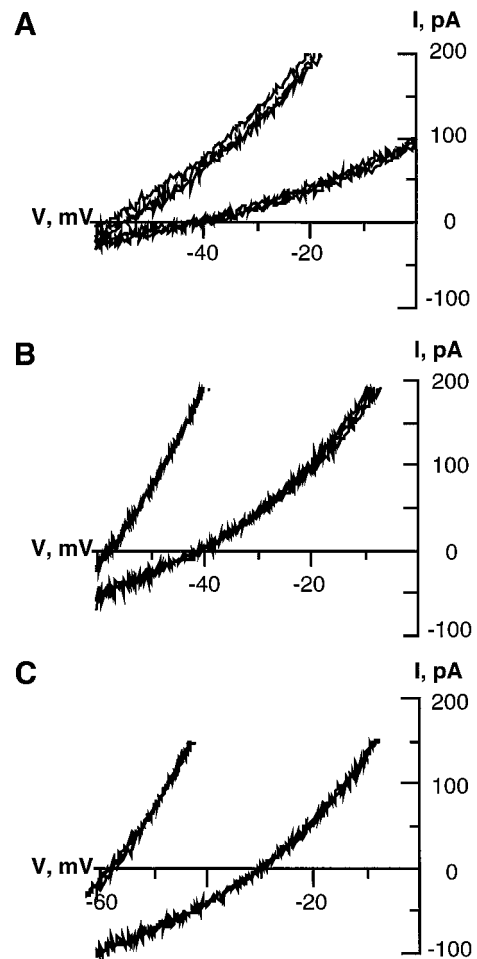


FIGURE 3 Current-voltage relationship comparing different MFR. (*A*) Volume-regulated anion current was developed at MFR = 0.4.  $V_R = -40$  mV when the current was stable. The extracellular solution was then changed to MFR = 0.00, with a corresponding change in  $V_R = -57$  mV. (*B*) Similarly, in a different cell,  $V_R = -40$  mV when current development stabilized in an extracellular solution of MFR = 0.80 and changed to  $V_R = -59$  mV with a change to MFR = 0.00. (*C*) Finally, in a third cell,  $V_R = -30$  mV when current development stabilized in an extracellular solution of MFR = 0.97 and changed to  $V_R = -58$  mV with a change in MFR = 0.00. All panels show three superimposed traces for each experimental condition.

were changed to MFR = 0.00. Once the solution change was complete, reversal potentials were stable. The intracellular ionic composition was constant and contained 120 mM aspartate and 0.2 mM Cl<sup>-</sup>. At high extracellular Cl<sup>-</sup> (MFR = 0.00), reversal potentials of the current in all three cells ranged between  $-57$  mV and  $-59$  mV, similar to the values reported in the literature (Jackson and Strange, 1993; Levitan et al., 1995; Lewis et al., 1993). Asp:Cl<sup>-</sup> permeability ratios, calculated from these reversal potentials using the GHK equation, range between 0.13 and 0.14. Reversal potential of the current at MFR = 0.40 (Fig. 3 *A*) is  $-40$  mV, yielding a higher asp:Cl<sup>-</sup> permeability ratio of 0.20. Reversal potentials at higher MFRs, however, yield much lower asp:Cl<sup>-</sup> permeability ratios. The values of the reversal potentials at MFRs of 0.80 and 0.97 are  $-40$  mV and

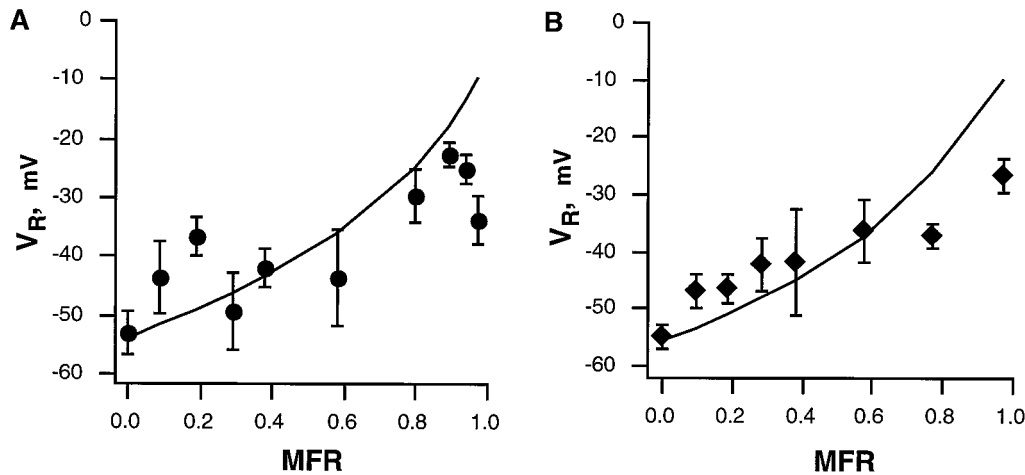


FIGURE 4 Dependence of reversal potential on MFR. (A) Reversal potentials measured in glut:Cl<sup>-</sup>-containing solutions. (B) Reversal potentials measured in asp:Cl<sup>-</sup>-containing solutions. Solid lines indicate expected reversal potential values calculated using the GHK equation, assuming independence of the MFR. The solid lines show the best visual fit to the data. Data points represent averages, with SEM shown as error bars (number of cells  $\geq$  5).

-30 mV (Fig. 3, B and C), yielding asp:Cl<sup>-</sup> permeability ratios of 0.08 and 0.014, respectively.

The dependence of the reversal potentials for volume-regulated anion current on extracellular MFRs of glut:Cl<sup>-</sup> or asp:Cl<sup>-</sup> ranging from 0.00 to 0.97 is summarized in Fig. 4, A and B, respectively. The intracellular ionic composition was constant and contained either glutamate or aspartate, as defined previously, in accordance with the extracellular ionic composition. With an extracellular MFR of 0.00, reversal potential of the volume-regulated current was  $-53.1 \text{ mV} \pm 3.6 \text{ mV}$  or  $-55.0 \text{ mV} \pm 2.2 \text{ mV}$  for cells recorded with the intracellular glutamate or aspartate, respectively. The solid lines in each part of Fig. 4 show theoretical reversal potential values calculated with the GHK equation, assuming that the permeability ratio ( $P_{aa}/P_{Cl}$ ) did not change with MFR. The best visual fits were

obtained for permeability ratios of 0.17 or 0.15 for glut:Cl<sup>-</sup> or asp:Cl<sup>-</sup>, respectively. Fig. 4 shows, however, that as the MFR increased, the data deviated further from the GHK expectation for both glutamate and aspartate mixtures.

Deviation from independence was clearly observed in the dependence of calculated permeability ratios on MFR. The values of the reversal potentials at MFR = 0.00 corresponded to permeability ratios of  $0.17 \pm 0.02$  and  $0.15 \pm 0.02$ , respectively (Fig. 5). The change in the permeability ratios was nonlinear and decreased as the MFR increased. At an MFR of 0.97,  $P_{\text{glut}}/P_{\text{Cl}}$  and  $P_{\text{asp}}/P_{\text{Cl}}$  were calculated to be  $0.012 \pm 0.003$  and  $0.02 \pm 0.003$ , respectively. Shifting the reversal potential to less depolarized voltages (-35 mV) by increasing the intracellular Cl<sup>-</sup> concentration but without changing the composition of the extracellular recording solutions did not cause a decrease in  $P_{aa}/P_{Cl}$ . This observa-

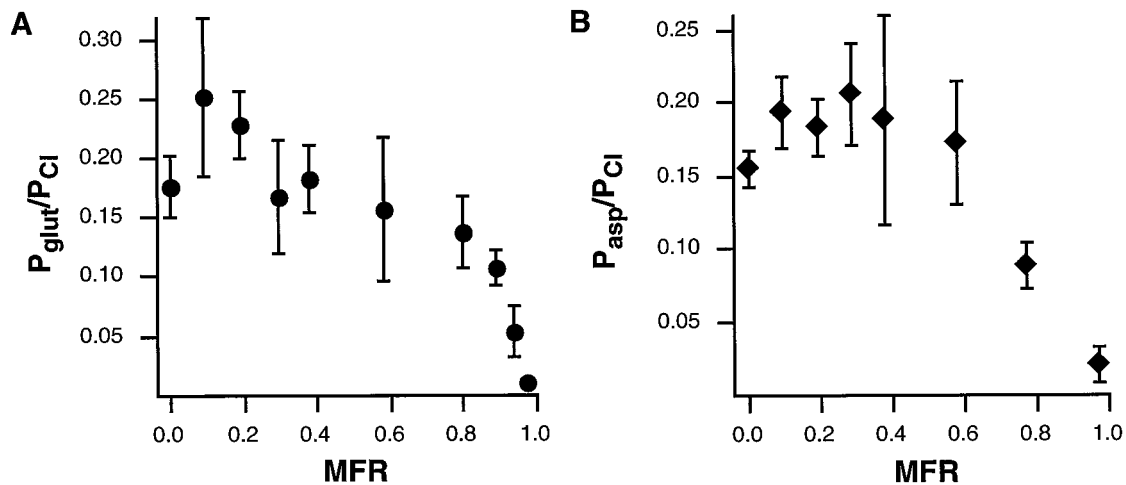


FIGURE 5 Dependence of permeability ratio on MFR. Permeability ratios were calculated from the data shown in Fig. 4, using the GHK equation (see Materials and Methods). (A) Permeability ratios calculated for glut:Cl<sup>-</sup>-containing solutions. (B) Permeability ratios calculated for asp:Cl<sup>-</sup>-containing solutions. Data points represent averages, with SEM shown as error bars (number of cells  $\geq$  5).

tion confirms that the observed shift in permeability ratio is due to the change in extracellular MFR and not to voltage sensitivity of the permeability ratios.

The shift in permeability ratios was fully reversible. Fig. 6 shows changes in reversal potentials and permeability ratios obtained from a cell that was first exposed to an extracellular solution of  $\text{asp}/\text{Cl}^-$  MFR = 0.00, then switched to MFR = 0.97, and then returned to a MFR = 0.00. Solution exchange was performed at a very slow rate to avoid changes in current activation due to the application of additional mechanical stimulus. A  $P_{\text{asp}}/P_{\text{Cl}}$  of 0.15 and 0.02 was calculated at MFR = 0.00 and 0.97, respectively. Permeability ratios calculated with  $\text{glut}:\text{Cl}^-$  solutions were similarly reversible (not shown). Thus the permeability ratio is highly dependent on the ionic composition of the solution, indicating that  $\text{Cl}^-$  and the anionic amino acids may interact within the pore of the volume-regulated channel.

The dependence of average current amplitudes on  $\text{glut}:\text{Cl}^-$  and  $\text{asp}:\text{Cl}^-$  MFRs are shown in Fig. 7, *A* and *B*, respectively. Solid lines represent the best fits obtained with

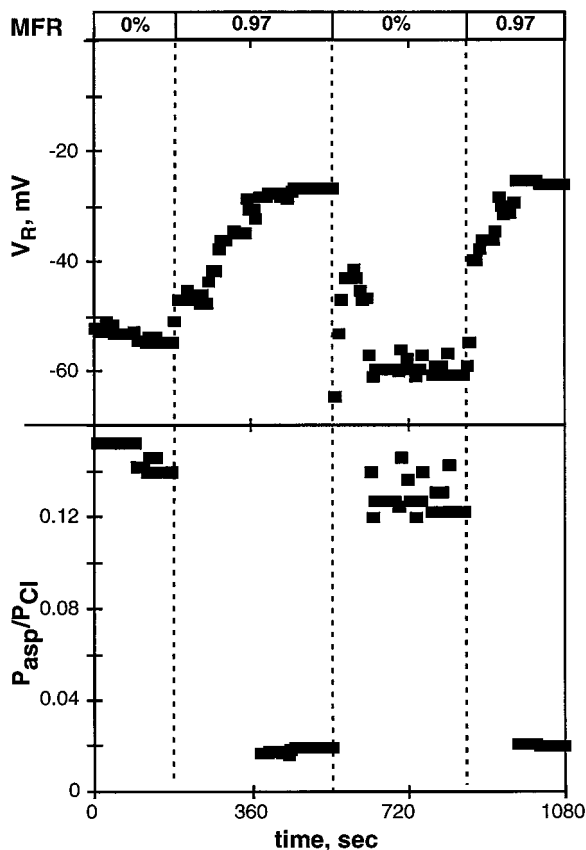


FIGURE 6 Dependence of  $P_{\text{asp}}/P_{\text{Cl}}$  on MFR was reversible. The composition of the extracellular solution was alternated by bath perfusion from MFR = 0.00 to MFR = 0.97 for two full cycles. Data shown were collected from a single cell. (Top) The change in the reversal potential with the change in extracellular ion composition. (Bottom)  $P_{\text{asp}}/P_{\text{Cl}}$ , calculated from reversal potentials shown in the top panel, varies with the change in ion composition.  $P_{\text{asp}}/P_{\text{Cl}}$  was calculated when bath perfusion ( $10\times$  chamber volume) was complete and reversal potential reached a stable value. Similar results were obtained in five cells.

the polynomial function of a third degree. Fits using this polynomial function produced a better fit to the experimental data than a linear function. For example, in glutamate-containing solution, the  $\chi^2$  calculated with the polynomial function was 0.044, whereas using a linear function to describe the data gave a  $\chi^2 = 0.066$ , indicating a worse fit with the linear function. Similarly, for aspartate-containing solutions, a polynomial fit gave  $\chi^2 = 0.043$ , whereas a linear function gave a  $\chi^2 = 0.085$ . Current amplitudes are expected to decrease linearly as amino acid/ $\text{Cl}^-$  MFR increases, if  $\text{Cl}^-$  and anionic amino acids permeate independently. In a multiion channel, however, current amplitudes may not decrease linearly (Hille, 1984).

### Possible contributions of other conductances

A dependence of  $\text{asp}:\text{Cl}^-$  permeability ratios on the extracellular MFR was observed only in cells that were challenged osmotically and developed an anion-selective conductance. A portion of cells ( $\sim 20\%$ ), however, when challenged osmotically, do not develop volume-regulated anion current as judged by 1) a lack of amplitude change when  $\text{Cl}^-$  is substituted with aspartate and 2) a lack of voltage-dependent inactivation. The observation that a portion of cells do not develop volume-regulated current has been reported before both by us (Levitan and Garber, 1995) and by others (Sole and Wine, 1991). A low-amplitude, outwardly rectifying nonselective cation current was occasionally observed in cells that were not challenged osmotically or did not develop volume-regulated anion current. The reversal potential of the nonselective cation current is  $1.8 \text{ mV} \pm 1.1 \text{ mV}$ .

Fig. 8 shows current-voltage relationships at MFR = 0.00 in a cell before (Fig. 8 *A*) and after (Fig. 8 *B*) development of volume-regulated anion current. Fig. 8 *A* shows current traces recorded 5 min after the transmembrane osmotic gradient was established. The figure shows a low-amplitude, outwardly rectifying current with a reversal potential of 0.0 mV, similar to a nonselective cation current that was typically recorded at isosmotic conditions. This current has no voltage-sensitive inactivation (Fig. 8 *A*, inset). Fig. 8 *B* shows traces of the current recorded from the same cell after volume-regulated anion current developed (15 min after the transmembrane osmotic gradient was established). Once the current developed, the value of the reversal potential became  $-55 \text{ mV}$ , indicating anion selectivity, and the current developed characteristic voltage-sensitive inactivation (Fig. 8 *B*, inset). This experiment shows that nonselective cation current may be easily distinguished from volume-activated anion current. If nonselective cation current contributed significantly to the measured reversal potentials, we would expect that the measured reversal potentials would be more depolarized than the true reversal potential and that the estimated  $\text{asp}:\text{Cl}^-$  permeability ratios would be higher than the true values of the permeability ratios. As the contribution of the nonselective cation current is expected to be more significant at low  $\text{Cl}^-$  concentrations (high MFR), it

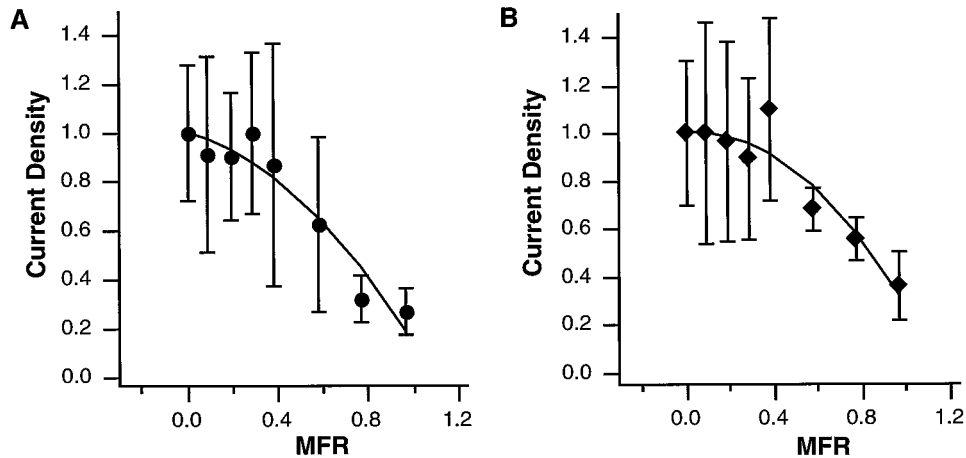


FIGURE 7 Dependence of volume-regulated current amplitudes on MFR. (A) Current amplitudes measured in glut:Cl<sup>-</sup>-containing solutions. (B) Current amplitudes measured in asp:Cl<sup>-</sup>-containing solutions. Current amplitudes were elicited by a voltage ramp from -60 to +100 mV (interpulse interval = 10 s) and measured at 100 mV. Current amplitude was normalized to a value measured at MFR = 0.00 and to initial cell capacitance. Data points represent the average of current density (pA/pF) measured from a single voltage ramp 5 min after the transmembrane osmotic gradient was established. Solid lines represent the best fit to a third-degree polynomial ( $y = 0.073 + 0.39x + 0.39x^2$  for glut:Cl<sup>-</sup> and  $y = 0.076 + 0.40x + 0.40x^2$  for asp:Cl<sup>-</sup>, where  $y$  is the normalized current density and  $x$  is the extracellular MFR ratio). See text for discussion. Data points represent averages, with SEM shown as error bars (number of cells  $\geq 5$ ).

may cause an apparent increase in the asp:Cl<sup>-</sup> permeability ratio as MFR increases. In contrast, our results show that as MFR increases, the value of the permeability ratios decreases. We conclude that the contribution of nonselective cation current does not have a significant effect on the observed anomalous mole fraction behavior of the volume-regulated anion current. A similar argument applies to the possible contribution of nonspecific leak currents. The reversal potential of a nonspecific leak current is necessarily 0 mV. Therefore, an increase in leak current at low Cl<sup>-</sup> concentrations will tend to drag the reversal potential closer to 0 mV, and in the direction opposite the one we observed.

## DISCUSSION

Ion permeation properties of the volume-regulated anion currents were studied to address the hypothesis that the

same ion channel pathway can be responsible for permeation of inorganic and organic osmolytes in hyposmotic challenged cells. This hypothesis is based on pharmacological similarities between volume-regulated currents carried by Cl<sup>-</sup> ions and by anionic amino acids (Kirk and Kirk, 1993; Roy and Malo, 1992). In this study, we show that volume-regulated currents carried by Cl<sup>-</sup>, aspartate, or glutamate develop after the cells are challenged with a transmembrane osmotic gradient. These currents have similar voltage-dependent inactivation, suggesting that the molecular identity of the ion channel underlying the current is the same (Levitan and Garber, 1995). The main finding of this study, that permeability ratios exhibit anomalous mole fraction behavior, indicates that permeant anions interact within the channel pore. This finding shows that Cl<sup>-</sup> and anionic amino acids may permeate through the same volume-regulated permeation pathway.

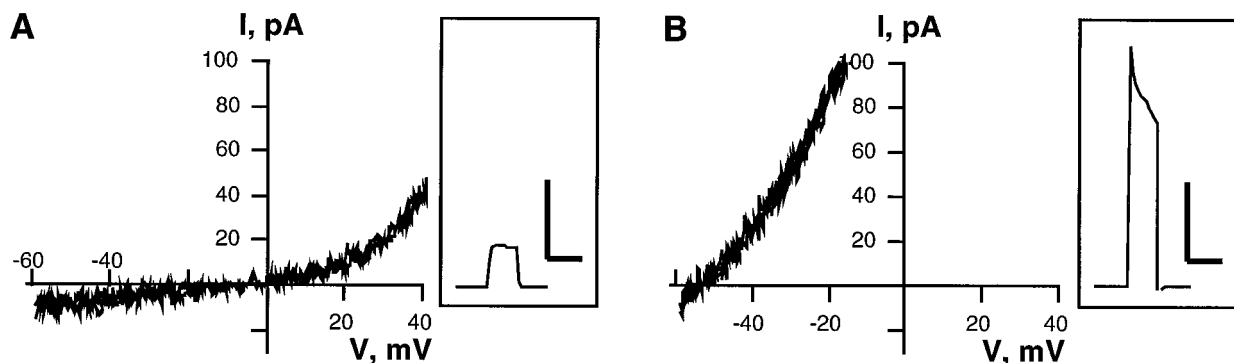


FIGURE 8 Change in  $V_R$  with volume-regulated anion current development. (A) The cell was challenged osmotically but did not develop significant anion current within 5 min of exposure. There was some development of nonselective current,  $V_R = 0$  mV, during this time, although there was no development of current inactivation (see inset). MFR = 0.00. (B) Anion current development in the same cell. Traces shown were taken 10 min after those shown in A. At this time  $V_R = -55$  mV, and the current shows voltage-dependent inactivation (inset). Each panel shows three superimposed traces. The scale bars in the insets represent 2 nA by 10 ms.

Volume-regulated fluxes of aspartate, glutamate, and taurine have been shown in osmotically challenged astrocytes and cortical neurons (Pasantes-Morales et al., 1993). Single-channel currents have been recorded using aspartate or glutamate as the charge carriers (Banderali and Roy, 1992). Taurine current has been recorded, but at a nonphysiological pH (pH 8.2), at which the amino acid is ionized (Banderali and Roy, 1992; Jackson and Strange, 1993). Recently, whole-cell currents have been recorded from pH 8 to pH 10 for 10 amino acids (Roy, 1995). Our results show directly that the anionic amino acids, aspartate and glutamate, and  $\text{Cl}^-$  ions can use the same volume-regulated anion conductance as a permeation pathway. Permeation pathways for other, nonanionic amino acids have yet to be established and are likely to be distinct from this volume-regulated anion conductance.

### Volume-regulated anion current: a permeation model

The molecular identity of this volume-regulated current is not known. Consequently, it is not possible to make predictions concerning relationships between identified amino acid residues and ion permeation. To gain further understanding of ion permeation mechanisms underlying volume regulation, we analyzed our results in terms of Eyring rate theory to approximate the experimental results reported here. Eyring rate theory describes the passage of a permeant ion through a pore by a series of energy barriers (transition states) and wells (ion binding sites). Computational models of ion permeation through a multiion channel show that different choices of energy profiles of wells and barriers may result in MFR-dependent permeability ratios and current amplitudes (Eisenman and Alvarez, 1991; Hille and Schwarz, 1978). Finding an energy profile that describes our experimental observations will allow us to make a prediction of the behavior of volume-regulated anion current as intracellular anions are depleted during the regulatory volume decrease.









We started by defining the various parameters that would be used to fit the data presented here. The first criterion was outward rectification of the current-voltage relationship under symmetrical  $\text{Cl}^-$  conditions (Levitan et al., 1995; Lewis et al., 1993). The second criterion was the dependence of the permeability ratio on MFR. Third, we defined our initial reference point (MFR = 0.00) as having a permeability ratio of  $P_{\text{aa}}/P_{\text{Cl}} = 0.16$  to conform to our experimental data. Using these criteria, both two-site and three-site energy profiles gave qualitatively similar results. We have chosen to use a four-barrier, three-well model, however, because this type of model gives a better fit to the experimental MFR data.

A rectification ratio of the volume-regulated anion current in symmetrical  $\text{Cl}^-$  solutions can be defined as current amplitude at +60 mV divided by the current amplitude at -60 mV. For this current, the value of this rectification

ratio was  $2.8 \pm 0.3$ . We found that the highest barrier for  $\text{Cl}^-$  must be toward the inside of the membrane to satisfy the criterion of outward rectification. An example of a good fit for the data was found in a  $\text{Cl}^-$  profile, where the peaks of the barriers are 15, 1, 1, 1 (as shown in Table 1, profiles I, III, and IV). The rectification ratio calculated for these parameters is 3.2, similar to the experimental value. The rectification ratio decreases if the relative height of the highest peak compared to the lower peaks decreases (e.g., a profile in which peak heights 3, 1, 1, 1 give a rectification ratio of 2.0). If, however, the highest peak is moved one step closer to the outside of the membrane (e.g., profile II, Table 1), the rectification ratio decreases to 1.5.

Table 1 shows the results of four different permeation profiles. Each profile satisfies our first criterion for predicting an outwardly rectifying current-voltage relationship. Each profile has a single high-energy barrier with equivalent energy wells. The difference among these four profiles is the relative position of the highest barrier for each permeant ion. The relative position of the highest barrier of each permeant ion was most critical in predicting an anomalous mole fraction effect. In the first two examples, profiles I and II, the highest barrier for each permeant ion is in the same position along the voltage drop across the membrane (Table 1).  $P_{\text{aa}}/P_{\text{Cl}}$  derived from profile I or II does not change with a changing MFR. Although Eyring rate profiles are not unique solutions, given our starting criteria, we could not find conditions that predicted a decrease in the permeability ratio with an increase in the MFR when the

**TABLE 1** Energy profiles: predictions for  $P_{\text{aa}}/P_{\text{Cl}}$  dependence on MFR

	Energy profile		$P_{\text{aa}}/P_{\text{Cl}}$	
	Cl	Amino acid	MFR = 0.0	MFR = 0.97
I			0.16	0.16
II			0.16	0.16
III			0.16	0.10
IV			0.16	0.05

In each case the highest barrier peaks for both ions were adjusted such that  $P_{\text{aa}}/P_{\text{Cl}} = 0.16$  when MFR = 0.00. The positions of the barriers are evenly spaced along the energy profile with wells midway between the barriers ( $\delta_{\text{well}} = 0.25, 0.50, 0.75$ ). The left side of the energy profiles is intracellular and the right side is extracellular. The ion interaction factor was 1.0 for all calculations. Energy values for barriers are (in RT, from intracellular to extracellular): profile I ( $\text{Cl}^-$ ), 15,1,1,1; profile I ( $\text{AA}^-$ ), 16.85,1,1,1; profile II ( $\text{Cl}^-$ ), 1,15,1,1; profile II ( $\text{AA}^-$ ), 1, 16.85,1,1; profile III ( $\text{Cl}^-$ ), 15,1,1,1; profile III ( $\text{AA}^-$ ), 1,17.3,1,1; profile IV ( $\text{Cl}^-$ ), 15,1,1,1; profile IV ( $\text{AA}^-$ ), 1,1,1,18.7. The peak heights were varied to conform with the requirement that  $P_{\text{aa}}/P_{\text{Cl}} = 0.16$  at MFR = 0.00. Energy values for wells are  $0.00RT$  in all cases. Ionic composition is as defined in Materials and Methods.



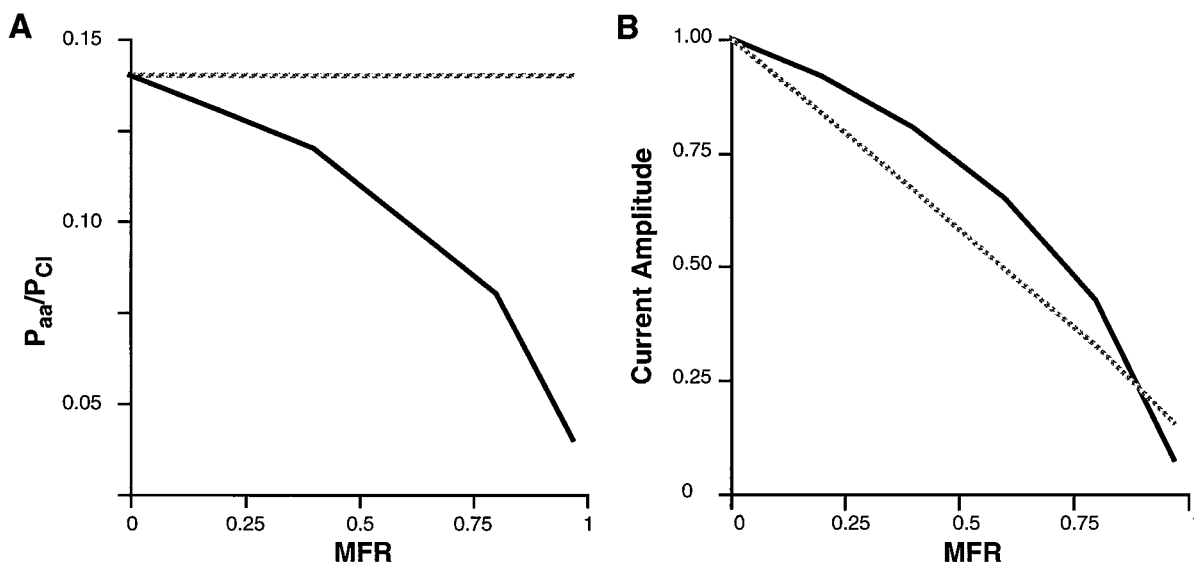


FIGURE 9 Predictions of amino acid and  $Cl^-$  permeation of volume-regulated current. (A) Predicted dependence of  $P_{aa}/P_{Cl}$  on MFR. (B) Predicted dependence of current amplitude on MFR. Solid lines represent Profile IV, and broken lines represent Profile I, as described in Table 1. Predictions from Profile IV exhibit anomalous mole fraction behavior, whereas those from Profile I do not. Parameters are as described in Table 1. Ionic compositions are as described in Materials and Methods. Current amplitude at 80 mV was normalized to that at MFR = 0.00.

highest barrier for each ion was in the same position along the voltage drop.

When the highest barrier for anionic amino acid permeation is moved toward the outer edge of the membrane, an anomalous MFR effect is predicted. Examples are shown in profiles III and IV in Table 1. A threefold decrease in  $P_{aa}/P_{Cl}$  at MFR = 0.00 and MFR = 0.97 is predicted as the highest barriers for  $Cl^-$  and amino acids are moved to each side of the membrane (profile IV, Table 1). Fig. 9 A shows the dependence of  $P_{aa}/P_{Cl}$  over the range of MFR = 0.00–0.97 as predicted by profiles I and IV. The decrease in  $P_{aa}/P_{Cl}$  is not linear and becomes significantly steeper at high MFRs, similar to that observed experimentally (e.g., Fig. 5). Profile IV also predicts a nonlinear dependence of current amplitude over the same MFR range (Fig. 9 B), which is again qualitatively similar to our experimental results (e.g., Fig. 7).

A model described by profile IV predicts that as intracellular  $Cl^-$  is depleted, the volume-regulated anion conductance becomes more permeable to anionic amino acids, thus allowing volume recovery to continue ( $P_{aa}/P_{Cl}$  increases from 0.09 to 0.13 when intracellular  $Cl^-$  concentration is decreased from 30 mM to 10 mM). This prediction is experimentally testable and will be addressed in our future studies. It is important to note, however, that profile IV is only an approximation of a permeation profile derived from a simple model of ion permeation. Increasing the complexity of the model will increase the approximation of the experimental results. For example, we compared energy profiles like that of profile IV for a two-binding-site and a three-binding-site pore. Increasing the number of binding sites along the energy profile for each permeant ion increases the dependence of  $P_{aa}/P_{Cl}$  on MFR. The permeabil-

ity ratio decreased from 0.16 to 0.065 in a two-barrier model, whereas it decreased from 0.16 to 0.05 in a three-barrier model.

### Volume-regulated ion permeation

What does interaction between permeant ions mean to volume regulation? The bottom line is that either  $Cl^-$  or anionic amino acids will flow through volume-regulated anion channels from the intracellular to the extracellular space in response to cell swelling and initiate regulatory volume decrease. A model defined by profile IV qualitatively describes our experimental observations for the anomalous mole fraction behaviors of both permeability ratios and current amplitudes. This model can be used to predict relative anionic permeabilities for a variety of physiological conditions. The recent work of Duan and colleagues (1997) suggests that ClC-3 protein is a volume-regulated anion channel, and that certain regions of this protein may be specifically involved in anion permeation. This finding may provide an inroad into testing for the role of multiion conduction in volume-regulatory responses.

We thank Dr. M. White, T. Begenisich, and D. Faber for critical reading of the manuscript. The "Barrier" software was a generous gift of Dr. T. Begenisich.

SSG is an Established Investigator of the American Heart Association. This work was supported by the National Institute of Diabetes, and Digestive and Kidney Diseases, National Institutes of Health (grant 46672), and the American Heart Association (grant 94002340).

## REFERENCES

- Banderali, U., and G. Roy. 1992. Anion channels for amino acids in MDCK cells. *Am. J. Physiol.* 263:C1200–C1207.
- Barry, P. H., and J. W. Lynch. 1991. Liquid junction potentials and small cell effects in patch-clamp analysis. *J. Membr. Biol.* 121:101–117.
- Begenisich, T., and M. D. Cahalan. 1980. Sodium channel permeation in squid axons. I. Reversal potential experiments. *J. Physiol. (Lond.)* 307:217–242.
- Begenisich, T., and C. Smith. 1984. Multi-ion nature of potassium channels in squid axons. *Curr. Top. Membr. Transp.* 22:353–369.
- Chamberlin, M. E., and K. Strange. 1989. Anisotonic cell volume regulation: a comparative view. *Am. J. Physiol.* 257:C159–C173.
- Deutsch, C., and S. C. Lee. 1988. Cell volume regulation in lymphocytes. *Renal Physiol. Biochem.* 3–5:260–276.
- Duan, D., C. Winter, S. Cowley, J. R. Hume, and B. Horowitz. 1997. Molecular identification of a volume-regulated chloride channel. *Nature* 390:417–421.
- Eisenman, G., and O. Alvarez. 1991. Structure and function of channels and channellogs as studied by computational chemistry. *J. Membr. Biol.* 119:109–132.
- Eyring, H., R. Lumry, and J. W. Woodbury. 1949. Some applications of modern rate theory to physiological systems. *Rec. Chem. Prog.* 10:100–114.
- Hamill, O. P., A. Marty, E. Neher, B. Sakmann, and F. J. Sigworth. 1981. Improved patch-clamp techniques for high-resolution current recording from cells and cell-free membrane patches. *Pflügers Arch.* 391:85–100.
- Haynes, J. K., and L. Goldstein. 1993. Volume-regulatory amino-acid transport in erythrocytes of the little skate, *Raja erinacea*. *Am. J. Physiol.* 265:R173–R179.
- Hille, B. 1984. *Ionic Channels of Excitable Membranes*. Sinauer Associates, Sunderland, MA.
- Hille, B., and W. Schwarz. 1978. Potassium channels as multi-ion single-file pores. *J. Gen. Physiol.* 72:409–442.
- Hoffman, E. K. 1992. Cell swelling and volume regulation. *Can. J. Physiol. Pharmacol.* 70:S310–S313.
- Jackson, P. S., and K. Strange. 1993. Volume-sensitive anion channels mediate swelling activated inositol and taurine efflux. *Am. J. Physiol.* 265:C1489–C1500.
- Kimelberg, H. K., E. Anderson, and H. Kettermann. 1990. Swelling-induced changes in electrophysiological properties of cultured astrocytes and oligodendrocytes. 2. Whole-cell currents. *Brain Res.* 529:262–268.
- Kirk, K., J. C. Ellory, and J. D. Young. 1992. Transport of organic substrates via a volume-activated channel. *J. Biol. Chem.* 267:23475–23478.
- Kirk, K., and J. Kirk. 1993. Volume-regulatory taurine release from a human lung cancer cell line. Evidence for amino acid transport via a volume-activated chloride channel. *FEBS Lett.* 336:153–158.
- Law, R. O. 1991. Amino acids as volume-regulatory osmolytes in mammalian cells. *Comp. Biochem. Physiol.* 99A:263–277.
- Law, R. O. 1994. Regulation of mammalian brain cell volume. *J. Exp. Zool.* 268:90–96.
- Levitan, I., C. Almonte, P. Mollard, and S. S. Garber. 1995. Modulation of a volume-regulated chloride current by F-actin. *J. Membr. Biol.* 147:283–294.
- Levitan, I., and S. S. Garber. 1995. Voltage-dependent inactivation of volume regulated  $\text{Cl}^-$  current in T84 and myeloma cells. *Pflügers Arch.* 431:297–299.
- Lewis, R. S., P. E. Ross, and M. D. Cahalan. 1993. Chloride channels activated by osmotic stress in T lymphocytes. *J. Gen. Physiol.* 101:801–826.
- McManus, M. L., and K. B. Churchwell. 1994. Clinical significance of cellular osmoregulation. In *Cellular and Molecular Physiology of Cell Volume Regulation*. K. Strange, editor. CRC Press, Boca Raton, FL. 63–80.
- Neher, E. 1992. Correction for liquid junction potentials in patch clamp experiments. *Methods Enzymol.* 207:123–131.
- Pasantes-Morales, H., S. Alavez, R. Sanchez-Olea, and J. Moran. 1993. Contribution of organic and inorganic osmolytes to volume regulation in rat brain cells in culture. *Neurochem. Res.* 18:445–452.
- Perez-Cornejo, P., and T. Begenisich. 1994. The multi-ion nature of the pore in Shaker  $\text{K}^+$  channels. *Biophys. J.* 66:1929–1938.
- Roy, G. 1995. Amino acid current through anion channels in cultured human glial cells. *J. Membr. Biol.* 147:35–44.
- Roy, G., and U. Banderali. 1994. Channels for ions and amino acids in kidney cultured cells (MDCK) during volume regulation. *J. Exp. Zool.* 268:121–126.
- Roy, G., and C. Malo. 1992. Activation of amino acid diffusion by a volume increase in cultured kidney (MDCK) cells. *J. Membr. Biol.* 130:83–90.
- Sanchez-Olea, R., J. Moran, A. Schousboe, and H. Pasantes-Morales. 1991. Hyposmolarity-activated fluxes of taurine in astrocytes are mediated by diffusion. *Neurosci. Lett.* 130:233–236.
- Solc, C. K., and J. J. Wine. 1991. Swelling-induced and depolarization-induced  $\text{Cl}^-$  channels in normal and cystic fibrosis epithelial cells. *Am. J. Physiol.* 261:C658–C674.
- Storck, T., S. Schulte, K. Hoffmann, and W. Stoffel. 1992. Structure, expression, and functional analysis of a  $\text{Na}^+$ -dependent glutamate/aspartate transporter from rat brain. *Proc. Natl. Acad. Sci. USA.* 89:10955–10959.